JACS
JOURNAL OF THE AMERICAN CHEMICAL SOCIETY

Communication

pubs.acs.org/JACS

Structure-Directing and High-Efficiency Photocatalytic Hydrogen Production by Ag Clusters

Yasser A. Attia,[†,‡] David Buceta,[†] Carmen Blanco-Varela,[†] Mona B. Mohamed,[‡] Giampaolo Barone,[∥] and M. Arturo López-Quintela*[,†]

[†]Physical Chemistry Department, Faculty of Chemistry, and NANOMAG Laboratory, University of Santiago de Compostela, E-15782 Santiago de Compostela, Spain

[‡]National Institute of Laser Enhanced Sciences, Cairo University, 12613 Giza, Egypt

[∥]Dipartimento di Scienze e Tecnologie Biologiche, Chimiche e Farmaceutiche, University of Palermo, I-90128 Palermo, Italy

Supporting Information

ABSTRACT: H_2 production by water splitting is hindered mainly by the lack of low-cost and efficient photocatalysts. Here we show that sub-nanometric silver clusters can catalyze the anisotropic growth of gold nanostructures by preferential adsorption at certain crystal planes of Au seeds, with the result that the final nanostructure can be tuned via the cluster/seed ratio. Such semiconducting Ag clusters are extremely stable and retain their electronic structure even after adsorption at the tips of Au nanorods, enabling various photocatalytic experiments, such as oxygen evolution from basic solutions. In the absence of electron scavengers, UV irradiation generates photoelectrons, which are stored within the nanorods, increasing their Au Fermi level up to the redox pinning limit at 0 V (RHE), where hydrogen evolution occurs with an estimated high efficiency of 10%. This illustrates the considerable potential of very small zerovalent, nonmetallic clusters as novel atomic-level photocatalysts.

Recent experiments have demonstrated that stable sub-nanometric metal clusters behave as semiconductors because of a bandgap which develops at the Fermi level,[1] giving rise to new properties such as photoluminescence[2,3] and magnetism.[4,5] It was found that the cluster bandgap increased with decreasing size of the cluster; the increase exceeded ∼2−3 eV for the smallest clusters reported so far.[6,7] Although the impressive catalytic activity of such small clusters has been predicted theoretically[8] and demonstrated experimentally by different groups (see, for example, refs 9−15), their use as structure-directing catalytic agents and demonstration of their possible photocatalytic activity for water splitting have not yet been reported.

The synthesis of anisotropic nanostructures by chemical methods is one of the major achievements of colloid science in recent decades,[16] and it has led to important new technological developments, such as plasmon-enhanced optical and opto-electronic devices,[17] as well as applications in sensing,[18] imaging, and biomedicine.[19] Among these developed colloidal methods, the seed-mediated approach is one of the simplest and most versatile avenues to large-scale synthesis of Au metal nanostructures having controlled size and shape. Although much experimental and theoretical work has been described since the first report by Murphy's group[16] about the influence of Ag salts on the final shape of the Au nanostructures, the detailed and complex mechanisms involved in such processes remain largely uncertain.[20,21] Previous studies have demonstrated the influence of different capping agents on the final structure and size of nanoparticles and have pointed to the major role of preferential adsorption (of surfactants, Ag, etc.) at specific crystal planes in inhibiting nanoparticle growth at such planes, giving rise to the formation of nanorods, nanotriangles, etc., depending on the amount of Ag salt used in the synthesis. However, minor variations in the solvent, counterions, reactants, and impurities have as yet unexplained major influences on the final products.[22] In this Communication, we will show that sub-nanometric Ag clusters are formed when Ag salts are used and can represent one possible missing link in this complex behavior, because they behave as structure-directing catalysts, thus improving our understanding of the influence of Ag salts in the resulting Au nanostructures. Moreover, it will be shown that such Ag clusters, adsorbed onto preferential planes of the formed Au nanostructures, are extremely stable and retain their semiconductor properties, as revealed by different photocatalytic properties displayed by such metal−cluster nanostructures. Gold nanorods (GNRs) are assumed to have adsorbed Ag clusters at the tips according to the previously mentioned structure-directing mechanism, and so (1) they are photodissolved by low-energy UV light, (2) such photodissolution can be inhibited using ethanol as hole scavenger, and (3) in the absence of oxygen (electron scavenger), they can generate photoelectrons, which are stored in the GNRs, increasing their Fermi level until they are pinned by the H^+/H_2 redox couple, with the subsequent high-efficiency production of hydrogen without the use of any other catalyst.

In a first set of experiments, we explored the influence of different concentrations of Ag ions and seed particles on the shape of the Au nanoparticles (details of the materials, characterization, and experimental conditions are given in the Supporting Information). Figure 1a−d shows the evolution of nanoparticle shape with the concentration of $AgNO_3$ (Figure

Received: October 11, 2013
Published: January 10, 2014

   dx.doi.org/10.1021/ja410451m | J. Am. Chem. Soc. 2014, 136, 1182−1185

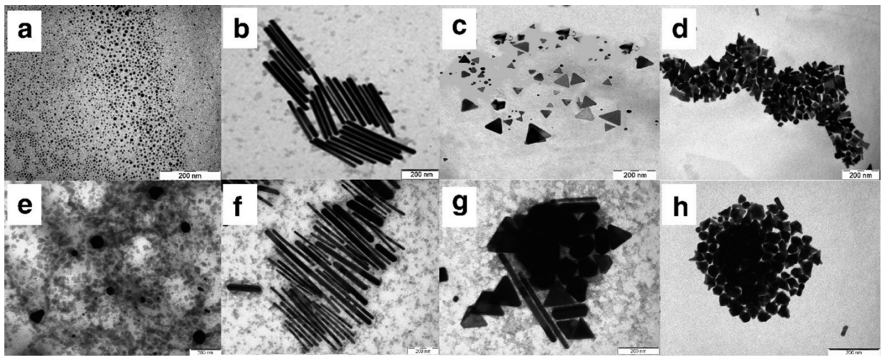

Figure 1. (Top) TEM images of Au nanoparticles produced with the same amount of Au seeds (50 nM) and different concentrations of $AgNO_3$: (a) 0, (b) 60, (c) 125, and (d) 300/900 μM. (Bottom) TEM images of Au nanoparticles produced with the same amount of Au seeds (48 nM) and increasing concentrations of Ag clusters: (e) 0, (f) 48, (g) 128, and (h) 950 nM.

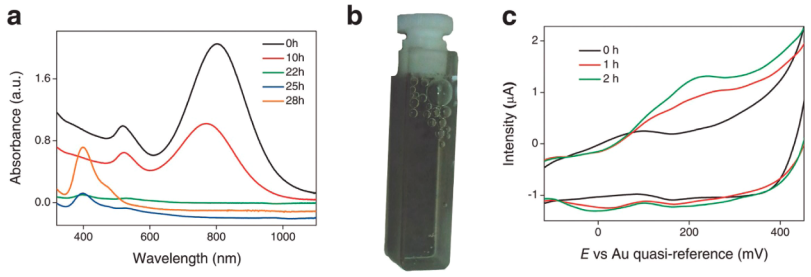

Figure 2. (a) Absorption spectra showing the changes of GNRs at pH 3.9 after irradiation under UV light for ~30 h, leading to complete decomposition of the rods and formation of Au(III)−CTAB complex, as evidenced by the appearance of its characteristic band at 398 nm (see Figure S9d). (b) Picture of the cell containing the solution, clearly showing the hydrogen bubbles produced after irradiation. (c) Cyclic voltammogram of a solution of GNRs at pH 3.9 with ethanol (1:1 in volume) under N_2 atmosphere without irradiation (black curve) and after the solution was irradiated for 1 h (red curve) and 2 h (green curve), showing that the hydrogen oxidation peak at around 0.2 V (Au quasi-reference, see Figure S13) appears only after irradiation of the sample.

S1 shows the corresponding changes in the absorption spectra). There is clearly an effect of the ratio of Ag ion concentration to seed concentration (R_{Ag} = [Ag^+]/[Au-seeds]) on the final shape of the Au nanoparticles (see Table S1). A new set of experiments allowed us to further conclude that (1) nanoparticle growth is catalyzed (not inhibited!) by Ag ions (see Figure S2), and (2) sub-nanometric Ag_2 and Ag_3 clusters are formed in the growth solution after addition of ascorbic acid under the same experimental conditions (see Figures S3−S5 and Table S2).

A possible explanation for these results assumes that the formed Ag clusters are adsorbed onto particular surfaces of the Au seeds, which can then act as catalysts, enhancing the growth of the GNRs. As noted above, metal clusters are widely recognized as singularly efficient catalysts,[10−12] as illustrated schematically in Figure S6. Gold particles, having a cubic lattice, tend to form cubes or spheres, because in those cases all facets tend to grow at the same rate (the result obtained in the absence Ag^+ ions). However, adsorption of Ag clusters on one of these facets (preferentially on {111} facets, see below) leads to breaking of the growth symmetry, causing that particular facet to grow much faster than the others. This leads to the formation of rod-shaped particles. HR-TEM analysis of GNRs (see Figure S7) shows the presence of {111} planes at the tips, which implies the preferential adsorption of clusters onto {111} planes. By increasing the Ag^+ concentration, more clusters are formed, which would be adsorbed on more than one facet, thus inducing the formation of new anisotropic shapes. The preferential adsorption on the {111} facet also implies a stronger adsorption, meaning that catalysis on these facets will be more difficult than on others because the clusters have to adsorb/desorb (see below). If we define $R_{GNRs} = R_{Ag}/(R_{Ag}$ for GNRs), then we observe that the formation of nanotriangles occurs when $R_{GNRs} \approx 2.5$ (see Table S1). Increasing further the Ag^+ ion concentration leads to the formation of multipods at $R_{GNRs} \approx 5$. Finally, with increasing concentration of Ag^+, growth occurs in all directions because clusters are adsorbed onto all crystal planes, leading to the formation of Au aggregates at $R_{GNRs} \approx 15$. In order to confirm this mechanism, we conducted a series of experiments in which externally prepared, well-defined clusters were employed instead of Ag^+ ions. For this purpose, small Ag clusters supplied by Nanogap (NGAP AQC Ag-1102-W), which were characterized previously and have been shown to be highly active for the electrocatalytic oxidation of alcohols,[23] were utilized. As can be seen in the complementary characterization of these clusters' samples (see Figure S8 and characterization details in the SI), Ag_3 is the most abundant cluster, which is one of the clusters detected in the experiments with Ag^+ ions (see above). Using a concentration of seeds similar to that in the previous experiments with Ag^+ ions (48 nM), another set of experiments was carried out using various quantities of Ag clusters. It can be seen from Figure 1f that, when the concentration of Ag_3 clusters is similar to that of seeds (48 nM, $R_{cluster}$ = [Ag-clusters]/[Au-seeds] ≈ 1), the resulting particles are rod-shaped, and the yield is about 95%. The aspect ratios were even larger than those obtained using Ag^+ ions (Figure 1b). Similarly, increasing the concentration of Ag clusters leads to formation of triangles ($R_{cluster} \approx 2.7$; Figure 1g) and finally multipods/aggregated particles ($R_{cluster} \approx 6−20$; Figure 1h).

dx.doi.org/10.1021/ja410451m | J. Am. Chem. Soc. 2014, 136, 1182−1185

Scheme 1. Schematic Energy Diagram Illustrating the Photodissolution of GNRs with Metal Clusters and Other Photocatalytic Processes[a]

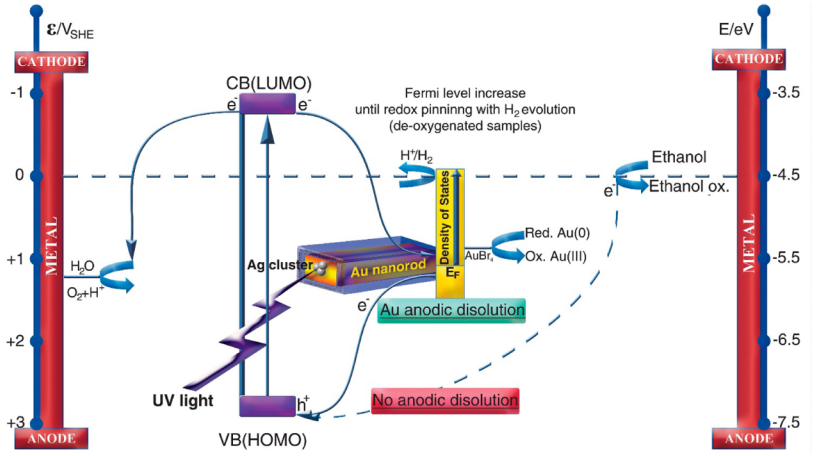

[a]Ethanol photo-oxidation and Fermi level increase in deoxygenated samples (in the presence of ethanol as sacrificial agent) up to its redox pinning limit at ε = 0 V (RHE), where hydrogen evolution occurs.

These findings are in good agreement with the results obtained using Ag^+ ions (see Table S1), the only difference being that the concentration of Ag^+ ions required to achieve the same anisotropy control is about 3 orders of magnitude larger than the concentration of clusters, due to the fact that not all Ag^+ ions are efficiently transformed into catalytic clusters. This clearly confirms that anisotropic growth is catalyzed and directed by Ag_3 clusters.

Having demonstrated the influence of cluster catalytic activity on anisotropic growth of nanoparticles, we now describe how the semiconducting properties assumed for Ag_3 clusters, with a bandgap of ~3.5 eV,[23] are retained when they are adsorbed onto the Au crystal planes, as it was assumed in the GNR formation mechanism. For this purpose, a sample of GNRs (pH ~3.9) was UV-irradiated (at a controlled temperature of 25 °C) using a low-intensity UV lamp at 254 nm, which is close to the excitation maximum of Ag_3 clusters (225 nm; see Figure S8d). Gradual decomposition of GNRs was observed (see Figure 2a), as deduced from the decreased amplitude of the characteristic plasmon absorption bands. It was observed that the rods decomposed, first forming spheres (see Figure S9b,c) and then completely disappearing after about 30 h of UV irradiation. Both the longitudinal and the transverse plasmon bands disappeared, and a new band appeared at 398 nm with a small shoulder at 475 nm, characteristic of the Au(III)−CTAB complex (see Figure S9d), indicating the complete oxidation of the GNRs (faster dissolution was achieved by stirring the samples, as can be seen in Figure S10a). Although Au metal is completely oxidized under UV radiation, Ag clusters remain stable in the solution even after the complete dissolution of the GNRs, as can be demonstrated by adding more ascorbic acid and seeds to give again GNRs (see Figure S10b). One way to ratify the adsorption of Ag clusters onto the GNRs is by observing the quenching of the cluster fluorescence in the presence of GNRs (see Figure S11). Another way is to eliminate the Ag clusters prior to irradiation. Clusters fuse in solution dispersions at temperatures of 120−150 °C, as can be seen by heating a cluster sample and detecting the formation of nanoparticles via the emergence of the plasmon band (results not shown here). Accordingly, a sample was heated to 130 °C for a period of 2 h, which greatly inhibited the photocorrosion process (Figure S12a). Photocorrosion occurs again when external Ag clusters are added (Figure S12b). A similar inhibition of the photodissolution was observed when GNR samples were repeatedly washed with distilled water prior to irradiation (see Figure S13). This suggests that the clusters are physisorbed onto the crystal planes of the GNRs, in line with their assumed role as structure-directing catalytic agents. Further confirmation of the presence of clusters on the GNRs was obtained by XANES, which will be published in a forthcoming paper. It is important to note that photodissolution is observed to begin at the tips of the GNRs because the longitudinal plasmon band disappears first.

The UV photodissolution of GNRs is, in principle, a surprising and unexpected result, because it is well known that Au is a noble metal, which appears not to be oxidized by UV light. However, one can understand these results by taking into account the semiconducting behavior of the Ag clusters, which are adsorbed primarily at the tips of the nanorods. DFT theoretical calculations strongly support the assumption that clusters do not lose their fundamental properties when they attach to Au seeds (catalyzing the formation of different Au nanostructures) or to Au metal nanorods (photocatalyzing different reactions; see theoretical studies in the SI). Therefore, Au atoms, located mainly at the tip surface of the GNRs at which the clusters are adsorbed, will be first oxidized by the highly oxidizing photoinduced holes produced by UV irradiation of the semiconducting Ag clusters, as shown in Scheme 1. This explains the photochemical dissolution of the GNRs. To visualize this dissolution phenomenon, one can consider the adsorption of clusters at the surface as a dynamic process, in which the CTAB-stabilized clusters are attached/detached to/from the Au surface. In order for the catalytic behavior reported above to occur without the clusters being incorporated (swallowed) into the Au lattice, the CTAB itself would have to mediate the formation of rods. Clusters would then be continuously adsorbed/desorbed at the preferential planes of the continuously reshaping/dissolving GNRs. In order to confirm and further explore this photocatalytic behavior of clusters, we carried out several additional cluster-mediated photocatalytic experiments. From Scheme 1, one

dx.doi.org/10.1021/ja410451m | J. Am. Chem. Soc. 2014, 136, 1182−1185

would expect that the introduction of typical hole scavengers, such as ethanol, should also inhibit the photocorrosion, as indeed happens (see Figure S14). Moreover, when the sample is deoxygenated (to avoid electron scavengers) and irradiation is carried out in the presence of a hole scavenger such as ethanol, the dissolution is profoundly inhibited. In this case, without electron scavengers in the system, the Au Fermi level of the GNRs can increase until it is pinned by the redox pair H^+/H_2. At that moment, H_2 is produced, as evidenced by the formation of bubbles on the sides of the cuvette (see Figure 2b) after about 1 h of UV irradiation. The production of H_2 was electrochemical confirmed, as shown in Figures 2c and S15. (Further evidence of the presence of hydrogen was obtained by using commercial equipment provided with a hydrogen-selective membrane; see SI methods.) After checking that Ag clusters without GNRs do not produce H_2, we confirmed that the H_2 production is mediated by the accumulation of electrons in the GNRs by observing a blue shift of the longitudinal surface plasmon resonance of irradiated GNRs in the absence of O_2 (Figure S16).[25] Preliminary calculations estimate an efficiency of H_2 production around 10% using 0.43 μg of clusters, which is an extraordinary high value, taking into account that the photocatalytic process is not optimized at all (see SI). All these results confirm that, indeed, clusters behave as atomic-scale quantum dots, which can be used as efficient atom-level photocatalysts for the production of hydrogen without any other specific catalyst.

In conclusion, we have shown that sub-nanometric, semiconducting Ag_3 clusters play an important role in the directed catalytic growth of different types of nanostructures. The formation of such clusters can be envisioned in terms of small amounts of metal ions present in reagents, solvents, and surfactants, employed for the synthesis of metal nanoparticles, which may account for the considerable sensitivity of anisotropic growth to the purity and even the source of the chemicals employed.[22] We have further shown that such catalytic clusters, attached to preferred planes of the nanostructures, remain stable and can be used as very efficient photocatalysts for the production of hydrogen. Because of the atomic scale of these quantum dots, several problems associated with the recombination of electron and holes (such as bulk and surface impurities and interface mismatching[24,26]), which diminishes the photocatalytic efficiencies in common semiconductors, could be avoidable. This opens up a novel broad new area of application of metal(0) clusters as atomic-scale quantum dots for high-efficient energy harvesting.

■ ASSOCIATED CONTENT

Supporting Information

Materials, methods, and additional figures. This material is available free of charge via the Internet at http://pubs.acs.org

■ AUTHOR INFORMATION

Corresponding Author

malopez.quintela@usc.es

Notes

The authors declare the following competing financial interest(s): M.A.L-Q. is scientific advisor of Nanogap. M.A.L-Q. and M.C.B. are stockholders of Nanogap.

■ ACKNOWLEDGMENTS

We want to acknowledge the financial support of the MCI, Spain (MAT2010-20442; MAT2011-28673-C02-01), MINECO, Spain (MAT2012-36754-C02-01), Xunta de Galicia (Grupos Ref. Comp., GRC2013-044, FEDER Funds), and Obra Social Fundación La Caixa (2012-CL097). Y.A.A. acknowledges a Ph.D. fellowship from the Egyptian Ministry of Education. G.B. acknowledges the allocation of computing resources by the CASPUR consortium through the Standard HPC Grant 2012.

■ REFERENCES

(1) Jin, R. *Nanoscale* **2010**, *2*, 343.
(2) Schaeffer, N.; Tan, B.; Dickinson, C.; Rosseinsky, M. J.; Laromaine, A.; McComb, D. W.; Stevens, M. M.; Wang, Y.; Petit, L.; Barentin, C.; Spiller, D. G.; Cooper, A. I.; Levy, R. *Chem. Commun.* **2008**, 3986.
(3) Haekkinen, H. *Chem. Soc. Rev.* **2008**, *37*, 1847.
(4) Moro, R.; Yin, S.; Xu, X.; de Heer, W. A. *Phys. Rev. Lett.* **2004**, *93*, 086803.
(5) Ledo-Suarez, A.; Rivas, J.; Rodriguez-Abreu, C.; Rodriguez, M. J.; Pastor, E.; Hernandez-Creus, A.; Oseroff, S. B.; Lopez-Quintela, M. A. *Angew. Chem., Int. Ed.* **2007**, *46*, 8823.
(6) Zheng, J.; Nicovich, P. R.; Dickson, R. M. *Annu. Rev. Phys. Chem.* **2007**, *58*, 409.
(7) Santiago Gonzalez, B.; Rodriguez, M. J.; Blanco, C.; Rivas, J.; Lopez-Quintela, M. A.; Martinho, J. M. G. *Nano Lett.* **2010**, *10*, 4217.
(8) Heiz, U.; Landman, U. *Nanocatalysis (Nanoscience and Technology)*; Springer: Berlin, 2007.
(9) Chen, W.-T.; Hsu, Y.-J.; Kamat, P. V. *J. Phys. Chem. Lett.* **2012**, *3*, 2493.
(10) Corma, A.; Concepción, P.; Boronat, M.; Sabater, M. J.; Navas, J.; Yacaman, M. J.; Larios, E.; Posadas, A.; López-Quintela, M. A.; Buceta, D.; Mendoza, E.; Guilera, G.; Mayoral, A. *Nat. Chem.* **2013**, *5*, 775.
(11) Vilar-Vidal, N.; Rivas, J.; López-Quintela, M. A. *ACS Catal.* **2012**, *2*, 1693.
(12) Oliver-Meseguer, J.; Cabrero-Antonino, J. R.; Domínguez, I.; Leyva-Pérez, A.; Corma, A. *Science* **2012**, *338*, 1452.
(13) Wei, W.; Lu, Y.; Chen, W.; Chen, S. *J. Am. Chem. Soc.* **2011**, *133*, 2060.
(14) Vajda, S.; Pellin, M. J.; Greeley, J. P.; Marshall, C. L.; Curtiss, L. A.; Ballentine, G. A.; Elam, J. W.; Catillon-Mucherie, S.; Redfern, P. C.; Mehmood, F.; Zapol, P. *Nat. Mater.* **2009**, *8*, 213.
(15) Bell, A. T. *Science* **2003**, *299*, 1688.
(16) Busbee, B. D.; Obare, S. O.; Murphy, C. J. *Adv. Mater.* **2003**, *15*, 414.
(17) Law, M.; Sirbuly, D. J.; Johnson, J. C.; Goldberger, J.; Saykally, R. J.; Yang, P. *Science* **2004**, *305*, 1269.
(18) Sudeep, P. K.; Joseph, S. T. S.; Thomas, K. G. *J. Am. Chem. Soc.* **2005**, *127*, 6516.
(19) Huang, X.; El-Sayed, I. H.; Qian, W.; El-Sayed, M. A. *Nano Lett.* **2007**, *7*, 1591.
(20) Liu, K.; Zhao, N.; Kumacheeva, E. *Chem. Soc. Rev.* **2011**, *40*, 656.
(21) Perez-Juste, J.; Pastoriza-Santos, I.; Liz-Marzan, L. M.; Mulvaney, P. *Coord. Chem. Rev.* **2005**, *249*, 1870.
(22) Smith, D. K.; Korgel, B. A. *Langmuir* **2008**, *24*, 644.
(23) Selva, J.; Martinez, S. E.; Buceta, D.; Rodriguez-Vazquez, M. J.; Blanco, M. C.; Lopez-Quintela, M. A.; Egea, G. *J. Am. Chem. Soc.* **2010**, *132*, 6947.
(24) Kamat, P. V. *J. Phys. Chem. C* **2008**, *112*, 18737−18753.
(25) Hirakawa, T.; Kamat, P. V. *J. Am. Chem. Soc.* **2005**, *127*, 3928.
(26) Sargent, E. H. *Nat. Photon.* **2012**, *6*, 133.